

New insight of time-transformed symplectic integrator I: hybrid methods for hierarchical triples

LONG WANG (王龙) ^{1,2}

¹*School of Physics and Astronomy, Sun Yat-sen University, Daxue Road, Zhuhai, 519082, China*

²*CSST Science Center for the Guangdong-Hong Kong-Macau Greater Bay Area, Zhuhai, 519082, China*

ABSTRACT

Accurate N -body simulations of multiple systems such as binaries and triples are essential for understanding the formation and evolution of interacting binaries and binary mergers, including gravitational wave sources, blue stragglers and X-ray binaries. The logarithmic time-transformed explicit symplectic integrator (LogH), also known as algorithmic regularization, is a state-of-the-art method for this purpose. However, we show that this method is accurate for isolated Kepler orbits because of its ability to trace Keplerian trajectories, but much less accurate for hierarchical triple systems. The method can lead to an unphysical secular evolution of inner eccentricity in Kozal-Lidov triples, despite a small energy error. We demonstrate that hybrid methods, which apply LogH to the inner binary and alternative methods to the outer bodies, are significantly more effective, though not symplectic. Additionally, we introduce a more efficient hybrid method, BlogH, which eliminates the need for time synchronization and is time symmetric. The method is implemented in the few-body code SDAR. We explore suitable criteria for switching between the LogH and BlogH methods for general triple systems. These hybrid methods have the potential to enhance the integration performance of hierarchical triples.

Keywords: N-body simulations (1083) — N-body problem (1082) — Multiple stars (1081) — Few-body systems (531)

1. INTRODUCTION

Observations have revealed that a significant fraction of stars form within multiple systems, including binaries, triples, and higher-order multiplicities (Sana et al. 2012; Duchêne & Kraus 2013; Moe & Di Stefano 2017; Gaia Collaboration et al. 2023; Donada et al. 2023; Offner et al. 2023). These systems play a crucial role in the long-term dynamical evolution of star clusters (e.g. Hénon 1961; Heggie 1975; Hills 1975; Heggie et al. 2006). Perturbed binaries can evolve into close interacting binaries and mergers, which may serve as progenitors of gravitational wave sources (Downing et al. 2010; Banerjee et al. 2010; Banerjee 2017, 2018, 2020, 2021; Tanikawa 2013; Antonini et al. 2014, 2017; Bae et al. 2014; Rodriguez et al. 2016a,b; Chatterjee et al. 2017; Askar et al. 2017; Fujii et al. 2017; Park et al. 2017; Samsing et al. 2018a; Samsing & D’Orazio 2018; Samsing et al. 2018b, 2024; Kremer et al. 2019; Di Carlo et al. 2019; Rastello et al. 2019; Kumamoto et al. 2019;

Fernández & Kobayashi 2019; Fragione & Loeb 2019; Antonini & Gieles 2020; Hong et al. 2020; Weatherford et al. 2021; Wang et al. 2021; Tiwari et al. 2024; Liu & Lai 2018, 2019; Randall & Xianyu 2018), as well as blue stragglers (Bailyn 1995; Lombardi et al. 1996; Hurley et al. 2001; Sills et al. 2005; Perets & Fabrycky 2009; Perets & Kratter 2012; Leigh et al. 2011; Hypki & Giersz 2013; Chatterjee et al. 2013; Alessandrini et al. 2016; Antonini et al. 2016; Fragione & Antonini 2019) and other exotic objects that generate significant astronomical interest.

Star-by-star numerical N -body simulations are commonly employed to study the dynamical evolution of star clusters and the formation of these objects. The simulations use an integrator to solve the equations of motion for N bodies under Newtonian forces, represented by a $6 \times N$ dimensional ordinary differential equation (ODE). However, accurately and efficiently integrating the orbits of multiple systems within star clusters presents significant challenges. Due to the inverse square law of Newtonian gravity, small time steps are necessary to accurately model the motions of stars as they approach each other. This situation is particularly prevalent in

highly eccentric binaries, close encounters, and chaotic multiple systems.

As multiple systems can complete a significant number of orbits during their lifetimes in star clusters, ODE solvers must also minimize cumulative integration errors to avoid artificially altering the energy and angular momentum of these systems. Such errors can lead to inaccurate predictions of binary evolution.

Moreover, the period distribution of multiple systems spans a wide range from days to Myrs, encompassing several magnitudes of timescales (e.g. Kroupa 1995). Tracking the orbital evolution of short-period multiple systems in long-lived massive star clusters, such as globular clusters, is time-consuming for classical ODE solvers.

Several solutions have been developed to address the challenges posed by multiple systems in star cluster simulations. The first solution employs a Kepler solver to track the orbital motion of binaries instead of directly solving the ODEs of Newtonian motion. This approach simplifies calculations by only requiring the orbital phase to be determined from parameters such as masses, semi-major axes, eccentricities, and times. The benefits include reduced computational cost and the elimination of cumulative errors and singularity issues associated with Newtonian forces. Gonçalves Ferrari et al. (2014) introduced a hybrid method using Keplerian-based Hamiltonian splitting and developed the SAKURA code, which uses a Kepler solver for two-body motions in N -body systems. Hernandez & Bertschinger (2015) developed a modified algorithm that is symplectic and reversible.

For multiple systems with one dominant central mass, Wisdom & Holman (1991) introduced a symplectic method (Wisdom-Holman method) that separates the Keplerian motion from perturbations by other bodies, allowing the application of a Kepler solver while using a second-order symplectic map for perturbations. Chambers (1999) expanded this concept by introducing a hybrid method that accommodates close encounters between massive bodies, leading to the development of the N -body code MERCURY, a state-of-the-art code for simulating the motion of planetary systems. Recent works by Rein et al. (2019) and Hernandez & Dehnen (2023) have further refined the switching criteria for this hybrid approach.

The secondary solution involves the use of the secular dynamical method for multiple systems (e.g. Ford et al. 2000; Eggleton & Kiseleva-Eggleton 2001; Fabrycky & Tremaine 2007; Hamers et al. 2015; Hamers & Portegies Zwart 2016; Hamers 2018, 2020). This method is par-

ticularly efficient for perturbed binaries in hierarchical triple and quadruple systems.

The third solution directly integrates the motion of multiple systems using a specially designed ODE solver. One such solver, introduced by (Kustaanheimo & STIEFEL 1965), transforms the equations of motion of a binary into a harmonic oscillation form to circumvent singularity. This method is applicable to perturbed binaries, and the state-of-the-art N -body code for star clusters, NBODY6, uses it (Aarseth 2003).

However, a drawback of these solutions is that they work well for hierarchical systems, where particle orbits can be approximately described by Keplerian dynamics, but they are not easily applicable to chaotic multiple systems. Another ODE solver capable of handling general multiple systems is the time-transformed symplectic method (Hairer 1997). Symplectic methods, such as LeapFrog integrators, conserve Hamiltonian during the integration of N -body systems. However, these methods require a constant time step, which can be inefficient for high-eccentric orbits and close encounters, as very small steps are needed to maintain accuracy when two bodies approach periapsis.

To address this, (Hairer 1997) introduced the time-transformed symplectic method, allowing the time step to vary according to a time transformation function. This flexibility enables adjustments to time steps according to the separation of two bodies, significantly enhancing the performance of the symplectic method. Preto & Tremaine (1999) developed an explicit time-transformed symplectic method with a specific time-transformation design, resulting in lower computational costs compared to implicit methods.

Additionally, Preto & Tremaine (1999) and Mikkola & Tanikawa (1999) introduced a logarithmic transformation within the explicit method, also known as algorithmic regularization, which can accurately trace the Kepler trajectory with only time phase errors. Wang & Nitadori (2020) provided mathematical proof of this feature, indicating that the logarithmic transformation yields a Kepler solver. We will henceforth refer to this method as the LogH method for convenience.

The LogH method has been implemented in several N -body codes for multiple systems, including ARCHAIN (Mikkola & Tanikawa 1999), SDAR (Wang et al. 2020b), MSTAR (Rantala et al. 2020), and TSUNAMI (Trani & Spera 2023). The basic LogH method employs a second-order drift-kick-drift map. To improve the accuracy of the integrator, the SDAR code uses a high-order symplectic method introduced by Yoshida (1990) with an optional adaptive step size controller, while the other three codes implement the Bulirsch-Stoer method. Al-

though the adaptive step size and the Bulirsch-Stoer method may disrupt the symplectic feature, they improve accuracy when evolving certain chaotic multiple systems. These codes also function as submodules in N -body codes for star clusters, such as NBODY7 (Aarseth 2003, 2012), AMUSE (Portegies Zwart et al. 2009), PETAR (Wang et al. 2020a), and BIFROST (Rantala et al. 2023).

Despite the success of the LogH method, in this work, we demonstrate that it is inefficient for hierarchical multiple systems due to the breakdown of the Kepler solver feature. In fact, accuracy significantly decreases even with a third body that has minimal perturbation on the binary. This issue has not been addressed in previous implementations of the method, primarily because the Bulirsch-Stoer method guarantees accuracy through iteration to a specified error tolerance. The low accuracy of the LogH method within the Bulirsch-Stoer framework results in poor performance with many adaptive iterations, masking the problem. Without a detailed investigation of the iteration process, identifying the low accuracy issue is difficult. Therefore, it is essential to investigate the time transformation function of the LogH algorithm to enhance its efficiency and accuracy for multiple systems.

In Section 2, we present the fundamental mathematical framework of the LogH method. Section 3 compares the integration of binary and triple systems, demonstrating a significant loss of accuracy for the latter when using the LogH method. In Section 4, we introduce hybrid methods that markedly enhance the accuracy of integrating triple systems. Section 5 discusses the switching criterion between the LogH and hybrid methods for general multiple systems with one inner binary. In Section 6, we evaluate why the hybrid method is superior and its limitations. Finally, Section 7 concludes with a discussion of remaining issues and future improvement plans.

2. THE MATHEMATICS OF THE LOGH METHOD

Preto & Tremaine (1999) provides the general formula for the explicit time-transformed symplectic method, which is constructed using the extended Hamiltonian of a Newtonian gravitational N -body system. The standard Hamiltonian for an N -body system is defined as

$$H(\mathbf{w}) = T(\mathbf{p}) + U(\mathbf{r}), \quad (1)$$

where $\mathbf{w} \equiv (\mathbf{r}, \mathbf{p})$, with \mathbf{r} and \mathbf{p} representing coordinates and momenta, and T and U denoting the kinetic and potential energy of all objects, respectively.

The extended Hamiltonian is defined as follows:

$$\Gamma(\mathbf{W}) = g(\mathbf{W}) [H(\mathbf{w}, t) - H(\mathbf{w}(0), 0)], \quad (2)$$

where $g(\mathbf{W})$ is a time-transformation function and \mathbf{W} is the extended phase-space vector. In this formulation, time t is treated as a coordinate, and the corresponding momentum is p_t initialized to $-H(\mathbf{w}(0), 0)$, representing the initial value of $-H(\mathbf{w}(0), t)$. We define the extended coordinate vector as $\mathbf{R} = (\mathbf{r}, t)$ and the extended momentum vector as $\mathbf{P} = (\mathbf{r}, p_t)$. The kinetic energy then includes p_t as $T(\mathbf{P}) = T(\mathbf{p}) + p_t$. Thus, $\Gamma(\mathbf{W})$ can be reformulated as

$$\Gamma(\mathbf{W}) = g(\mathbf{W}) [T(\mathbf{P}) + U(\mathbf{R})], \quad (3)$$

As t is treated as a coordinate, the equation of motion based on $\Gamma(\mathbf{W})$ is defined as

$$\frac{d\mathbf{W}}{ds} = \{\mathbf{W}, \Gamma(\mathbf{W})\}, \quad (4)$$

where $\{\}$ denotes the Poisson bracket, and s is a new differential variable replacing t .

A specific form of $g(\mathbf{W})$ introduced by Preto & Tremaine (1999) is given by

$$g(\mathbf{W}) = \frac{f(T(\mathbf{P})) - f(-U(\mathbf{R}))}{T(\mathbf{P}) + U(\mathbf{R})}, \quad (5)$$

which results in a separable Γ :

$$\Gamma(\mathbf{W}) = f(T(\mathbf{P})) - f(-U(\mathbf{R})), \quad (6)$$

allowing the use of explicit symplectic methods such as Leapfrog.

The explicit formulae of the equation of motion are given by

$$\begin{cases} \frac{d\mathbf{r}}{ds} = f'(T(\mathbf{p}) + p_t) \frac{\partial T(\mathbf{p})}{\partial \mathbf{p}} \\ \frac{dt}{ds} = f'(T(\mathbf{p}) + p_t) \\ \frac{d\mathbf{p}}{ds} = f'(-U(\mathbf{r}, t)) \frac{\partial U(\mathbf{r}, t)}{\partial \mathbf{r}} \\ \frac{dp_t}{ds} = f'(-U(\mathbf{r}, t)) \frac{\partial U(\mathbf{r}, t)}{\partial t}. \end{cases} \quad (7)$$

As demonstrated in Preto & Tremaine (1999) and Mikkola & Tanikawa (1999), when $f(x) = \log(x)$ and the drift-kick-drift Leapfrog method with a fixed step Δs (sDKD) are applied, the solution accurately follows a Kepler orbit. In this work, we refer to this as the LogH method. For isolated multiple systems with conservative potential, $U(\mathbf{r}, t)$ does not explicitly depend on t and p_t is constant. The drift and kick steps of the method are described as follows:

- Drift:

$$\begin{cases} \mathbf{r}_{k+\frac{1}{2}} = \mathbf{r}_k + \frac{\Delta s}{2} g_d|_{2k} \left. \frac{\partial T(\mathbf{p})}{\partial \mathbf{p}} \right|_{2k} \\ t_{k+\frac{1}{2}} = t_k + \frac{\Delta s}{2} g_d|_{2k} \\ k = 0 \text{ or } \frac{1}{2}, \end{cases} \quad (8)$$

- Kick:

$$\mathbf{p}_1 = \mathbf{p}_0 + \Delta s g_k|_{\frac{1}{2}} \left. \frac{\partial U(\mathbf{r})}{\partial \mathbf{r}} \right|_{\frac{1}{2}}, \quad (9)$$

where the two drift steps are represented by different k values, and

$$\begin{cases} g_d = f'(T(\mathbf{p}) + p_t) = \frac{1}{T(\mathbf{p}) + p_t} \\ g_k = f'(-U(\mathbf{r})) = -\frac{1}{U(\mathbf{r})} \end{cases} \quad (10)$$

represents the time transformation functions for the drift and kick steps, respectively. Notice that these functions differ from $g(\mathbf{W})$ in Equation 2.

In the drift step, time t is an integrated variable dependent on g_d . In a Kepler orbit, g_d is maximized and Δt is minimized at periapsis. Thus, the LogH method is better than the classical drift-kick-drift LeapFrog method with a constant time step Δt . From now on, we will refer to this classical method as tDKD, distinguishing it from the sDKD used in the LogH method.

In addition, as shown in [Preto & Tremaine \(1999\)](#) and [Wang & Nitadori \(2020\)](#), the LogH method functions as a Kepler solver that advances the eccentric anomaly E while keeping other orbital elements constant. Consequently, only the time integration is affected by the second-order approximation (truncation) error of the LeapFrog method, while the solution can exactly trace the Keplerian trajectory while experiencing round-off errors.

The integration step Δs has a physical interpretation, as the change in eccentric anomaly (ΔE) ([Wang et al. 2020a](#); [Wang & Nitadori 2020](#)):

$$\Delta s = \mathcal{L} \tan \frac{\Delta E}{2}, \quad (11)$$

where \mathcal{L} is the conjugate momenta of the mean anomaly, defined as:

$$\mathcal{L} = \sqrt{\frac{G(m_1 m_2)^2 |a|}{m_1 + m_2}}, \quad (12)$$

with a , e , m_1 , m_2 and G representing the semi-major axis, eccentricity, masses of two components, and gravitational constant, respectively. Thus, Δs has units of angular momentum. As Δs approaches infinity, ΔE equals π , indicating a traversal of half an orbit.

2.1. MA2002 method

[Mikkola & Aarseth \(2002\)](#) developed a time-transformed LeapFrog method, which is more general than the LogH method, although it may sacrifice symplecticity. This method defines two time-transformation functions for the drift and kick steps of the LeapFrog approach. During kick steps, the function is defined as:

$$g_k^{\text{MA}} = 1/\Omega(\mathbf{r}), \quad (13)$$

where $\Omega(\mathbf{r})$ is an arbitrary function of \mathbf{r} .

In drift steps, the function is defined as¹

$$g_d^{\text{MA}} = 1/u, \quad (14)$$

where u is a new integrated variable given by

$$\frac{du}{dt} = \frac{\partial \Omega(\mathbf{r})}{\partial \mathbf{r}} \cdot \mathbf{v}, \quad (15)$$

with \mathbf{v} representing the velocity vectors. Since u depends on $\Omega(\mathbf{r})$, it is calculated during the kick steps and used in the drift steps.

For conservative potential, we can set $\Omega(\mathbf{r})$ as $-U(\mathbf{r})$. In this case, the method (MA2002) approximates the LogH method. Here, g_k^{MA} is equivalent to the function g_k (Equation 10) of the LogH method. The corresponding u can be expressed in integral form²:

$$u = \int \frac{-\partial U(\mathbf{r})}{\partial \mathbf{r}} \cdot \mathbf{v} dt. \quad (16)$$

By setting the initial value of u to the initial value of $-U(\mathbf{r})$, we have $u \equiv -U(\mathbf{r})$. Due to energy conservation, $T(\mathbf{p}) + p_t = -U(\mathbf{r})$, u can be viewed as $T(\mathbf{p}) + p_t$. Thus, we can find that

$$\frac{1}{u} = \frac{1}{-U(\mathbf{r})} = \frac{1}{T(\mathbf{p}) + p_t}, \quad (17)$$

which is equivalent to g_d function (Equation 10) of the LogH method. However, in numerical simulations, $T(\mathbf{p}) + p_t \approx -U(\mathbf{r})$, making u an approximation of $T(\mathbf{p}) + p_t$.

Therefore, the MA2002 method can be viewed as the LogH method with g_d approximated by g_d^{MA} . The drift and kick steps can be described using the same Equations 8 and 9, with g_k defined as in Equation 10 and g_d replaced by Equation 14. The value of u can be calculated during kick steps as:

$$u_1 = u_0 - \Delta s g_k|_{\frac{1}{2}} \left. \frac{\partial U(\mathbf{r})}{\partial \mathbf{r}} \right|_{\frac{1}{2}} \cdot \left(\frac{\mathbf{v}|_0 + \mathbf{v}|_1}{2} \right), \quad (18)$$

¹ Here, u represents W as defined in Equation 12 of [Mikkola & Aarseth \(2002\)](#)

² The same definition of u in Equation 40 of [Wang et al. \(2020a\)](#) is missing a negative sign and dt .

with $\mathbf{v}|_1$ calculated in Equation 9. This formula approximates u assuming that $\partial U(\mathbf{r})/\partial \mathbf{r}$ is constant during one step.

The original LogH method is Δs symmetric or time symmetric because reversing Δs for backward integration yields the same formulae of integrated quantities (Equations 8 and 9). The MA2002 method retains this feature, including the additional integration of u in Equation 18. Thus, the MA2002 method also achieves good long-term behavior with respect to the cumulative energy error.

Due to approximation errors, the computation of g_d in the MA2002 method differs from the exact value in Equation 10. Consequently, the MA2002 method is less accurate than the original LogH method, especially for the Kepler orbits. The error differences between the two methods are detailed in the Appendix A. For isolated binaries, the original LogH method achieves better accuracy, with the Γ error mainly caused by round-off errors. In contrast, the MA2002 solution closely follows the Kepler trajectory, but exhibits some secular error patterns. However, both methods show similar accuracy for triple systems. Thus, the MA2002 method serves as a good approximation to the LogH method and adequately demonstrates its limitations in evolving hierarchical triples in the following sections.

In addition, due to flexible changes in $\Omega(\mathbf{r})$ and the definition of u in the MA2002 method, we use the MA2002 method to develop a new algorithm in this work. To ensure consistent comparisons among methods, the term ‘‘LogH method’’ will refer to the MA2002 method in the following content.

3. COMPARISON OF THE LOGH METHOD FOR BINARY AND TRIPLE SYSTEMS

The unique advantage of the LogH method for solving Kepler orbits does not extend to other multiple systems, such as triples. Using the SDAR code, we compare how the energy error varies with the step size Δs for an isolated binary and a hierarchical triple including a weakly perturbed binary. Figure 1 illustrates the configurations of the binary and triple systems.

Before detailing the results, we first introduce the model naming convention used throughout the following content. To represent values of Δs , we define a reference value, Δs_0 , which corresponds to one period of the binary. We then use the term ‘S’ followed by the division number to denote the different Δs values; for example, S16 represents $\Delta s_0/16$ and S64 represents $\Delta s_0/64$. For convenience, we sometimes append this designation as a suffix to the method name to indicate a simulation using that method with the specified Δs . For instance, LogH-

S16 denotes the simulation using the LogH method with $\Delta s = \Delta s_0/16$. To enhance accuracy, we occasionally employ the 6th-order Yoshida method (Yoshida 1990) in the sDKD and LogH components, indicated as ‘Y6’ in the model names, such as LogH-Y6-S16. This naming convention will be applied consistently throughout the following text.

We set the initial conditions of the binary with an eccentricity of $e = 0.9$, a semi-major axis of $a = 0.001$ and component masses of $m_1 = 0.9$ and $m_2 = 0.1$. For convenience, we use scale-free units with gravitational constant $G = 1$. This allows flexibility in scaling the binary to different astrophysical systems by defining two units, such as mass and distance. The corresponding period of this binary is approximately 2×10^{-4} . The choice of high e and unequal masses better demonstrates the ability of the LogH method to maintain accuracy at periapsis.

Starting at apoapsis, we integrate the binary orbit to $t = 0.001$, roughly five periods. The cumulative absolute (positive) energy error ϵ as a function of t is displayed in the left panel of Figure 2. We select three values of Δs : $1/16, 1/64$ and $1/256$ of Δs_0 for comparison. The result shows that ϵ is on the order of 10^{-13} and independent of Δs , demonstrating that the method traces the Kepler trajectory well. ϵ does not exactly reach the round-off error limit of 64-bit double precision. The reason is discussed in Appendix A.

For comparison, we set the initial conditions of the triple by adding a weak perturber to the binary with the same parameters. The perturber is ten times less massive than the lower-mass object in the binary ($m_3 = 0.01$) and orbits the binary in a circular path. The outer semi-major axis, $a_o = 10$, is 10^4 times larger than the inner one. Both the outer and inner orbits are coplanar with zero inclination.

In this setup, while the influence of the third body is weak, the integration results using the same Δs choices as in the isolated binary case exhibit significantly larger ϵ values depending on Δs , as shown in the right panel of Figure 2. The relationship $\epsilon \propto \Delta s^2$ indicates second-order accuracy. This suggests that even a weak perturber can disrupt the ability to trace Keplerian trajectories, reducing it to a standard second-order symplectic method.

The primary issue when applying the LogH method to triple systems is that the g_k includes two terms of potential energy from the third body:

$$g_k = f'(-U(\mathbf{R})) = \left[\frac{Gm_1m_2}{r_{12}} + \frac{Gm_1m_3}{r_{13}} + \frac{Gm_2m_3}{r_{23}} \right]^{-1}, \quad (19)$$

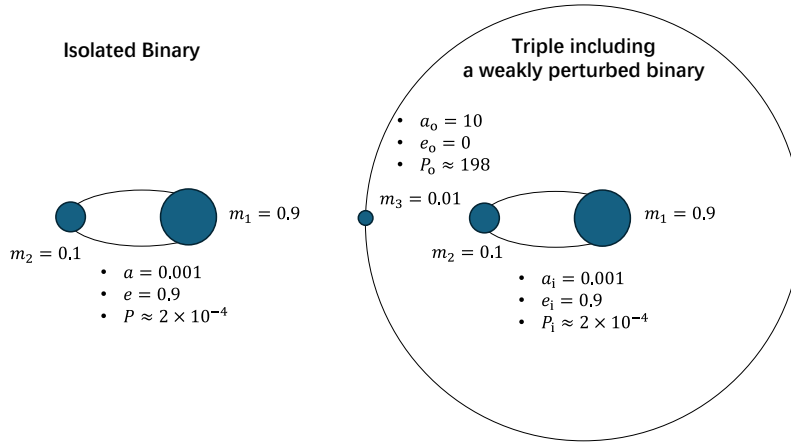


Figure 1. The diagram illustrates the initial conditions of the binary and triple for simulations. In the context of the triple system, the subscripts "i" and "O" in the orbital parameter symbols denote the inner and outer orbits, respectively. Note that there is a fourfold magnitude difference between a_o and a_i , and the outer circle and inner ellipse representing the outer and inner orbits of the triple do not reflect the true scale.

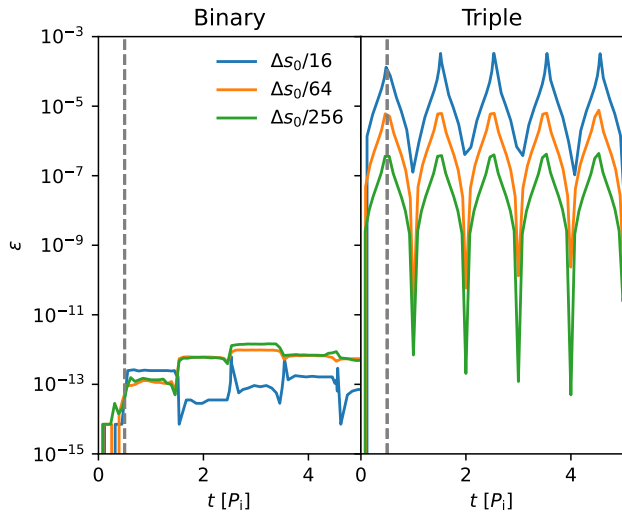


Figure 2. The energy error ϵ as a function of time for simulations of the binary (upper panel) and triple (lower panel) systems using the LogH method, with colors indicating Δs . The dashed vertical line indicates the time of periaapsis.

where r_{12} , r_{23} and r_{13} represent the separation between each pair of bodies. With these terms included, the LogH method cannot be regarded as a Kepler solver like integrator, thus undermining its benefit.

We can view this differently: in the case of an eccentric Kepler orbit, $g_k \propto r_{12}$. When the binary reaches periaapsis, g_k reaches its minimum value, resulting in the smallest Δt for a given constant Δs . This is reasonable because the acceleration between two bodies is maximized at periaapsis, necessitating a small time step for sufficient accuracy. However, with the presence of a third body, the additional potential terms in g_k smooth the variations of g_k , making Δt less sensitive to changes

in r_{12} of the inner binary. This can reduce the accuracy of integration at periaapsis.

4. HYBRID METHODS

4.1. *H4: Hermite and LogH*

The issue discussed can be avoided in a hybrid scenario. In N -body codes like NBODY7, SDAR and PETAR, the LogH method is combined with other integrators, such as 4th-order Hermite with block time steps, to form a hybrid method referred to as "H4". In this case, the LogH method is used for the inner binary, while another integrator manages the outer orbit. The influence of the third body on the inner binary is treated as a perturbative force during the kick step in the LogH method, allowing the ability to accurately approximate Keplerian trajectories to be preserved.

However, this hybrid method has a disadvantage. The primary bottleneck is that the time steps $\Delta t_{B,k}$ in the LogH method are quantities to integrate, making it difficult to design Δs to ensure integration completes at the required time Δt_H from the other integrator. As a result, additional iterative steps are necessary for time synchronization. If Δt_H is comparable to $\Delta t_{B,k}$, the hybrid method becomes time-consuming and accumulates timing errors from frequent synchronizations. If Δt_H exceeds the period of the inner binary, the interaction between the inner binary and the outer body occurs less than once per inner orbit, resulting in inaccurate evolution.

4.2. *BlogH: sDKD and LogH*

We introduce a new hybrid method "BlogH", which avoids time synchronization. In this approach, all objects in the triple are integrated using Equations 8 and 9, but the definitions of g_d and g_k are modified. In the

BlogH method, only the potential energy of the inner binary,

$$U_b = -\frac{Gm_1m_2}{r_{12}}, \quad (20)$$

is included in g_k as follows:

$$g_{k,b} = \frac{1}{-U_b}, \quad (21)$$

where new symbol $g_{k,b}$ distinguishes it from g_k in the LogH method.

Since g_k and g_d must represent the equivalent quantities to ensure consistent time steps for kick and drift, and considering total energy conservation, we have

$$T(\mathbf{p}) + p_t = -U(\mathbf{r}, t) = -U_b + [-U(\mathbf{r}, t) + U_b], \quad (22)$$

the corresponding $g_{d,b}$ in the BlogH method is given by:

$$g_{d,b} = \frac{1}{T(\mathbf{p}) + p_t + U(\mathbf{r}, t) - U_b}, \quad (23)$$

which depends on coordinates, making it unsuitable for the explicit method. The solution is to adopt a similar approach to that in Equation 16 to approximate $g_{d,b}$ by defining u_b as:

$$u_b = \int \frac{-\partial U_b}{\partial \mathbf{r}_b} \cdot \mathbf{v}_b dt \quad (24)$$

where \mathbf{v}_b includes only the inner binary components. This formula can be evaluated at kick steps following Equation 18. Then,

$$g_{d,b} = \frac{1}{u_b}, \quad (25)$$

which can be used in the explicit method.

This scenario enables the inner binary to be integrated with the LogH method, while the outer orbit is integrated with the sDKD method, following the same time-step sequences $\Delta t_{B,k}$ as the inner binary. This setup allows the third body to provide perturbations at the kick step without affecting the time transformation. The method retains the advantages of accurately approximating Keplerian trajectories without the need for time synchronization. The disadvantage is that the method is not symplectic due to the approximations in the MA2002 method and the unequal time steps of the sDKD loop for outer orbits. However, compared to the H4 method, BlogH is time symmetric. Figure 3 illustrates the differences in treatment in time steps among the three methods: LogH, H4 and BlogH.

The BlogH method can also be applied to hierarchical multiple systems that contain one innermost binary. For example, consider a hierarchical quadruple system with

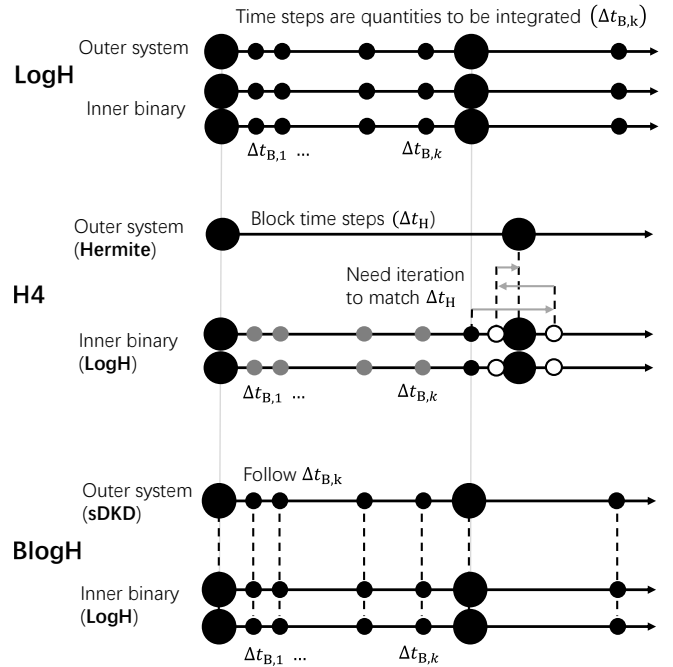


Figure 3. The illustration of three integration methods for time step treatment in a multiple system with one inner binary and outer bodies.

an inner binary with components 1 and 2, and two outer bodies, 3 and 4, which do not form a binary. The dynamics of the four bodies are integrated using Equations 8 and 9. However, only the innermost binary (components 1 and 2) is used to calculate $g_{k,b}$ and $g_{d,b}$ through Equations 21, 24 and 25.

Implementing the BlogH method in a LogH N -body code is straightforward. The only necessary modification is to update the functions g_d and g_k , while the overall framework of the integrator remains unchanged. We have incorporated the BlogH method into the SDAR code, alongside the existing LogH and H4 methods.

4.3. Triples including a weakly perturbed binary

To show that the hybrid methods outperform the LogH method, we redo simulations of the triple system including a weakly perturbed binary by using the LogH, H4 and BLogH methods with varying Δs . We evolve the triple system to 500 periods of the inner binary (P_1) to assess the secular evolution of energy and orbital elements.

In the triple system, since the outer orbit is circular, the time step of the Hermite part (Δt_H) can remain constant in the H4 method. According to the block time step scheme, we select $\Delta t_H = 0.5^{14} \approx 0.307P_1$ for the maximum Δs . When Δs is reduced by a factor of 4, Δt_H is halved to maintain consistent accuracy between the

second-order LogH method and the fourth-order Hermite method.

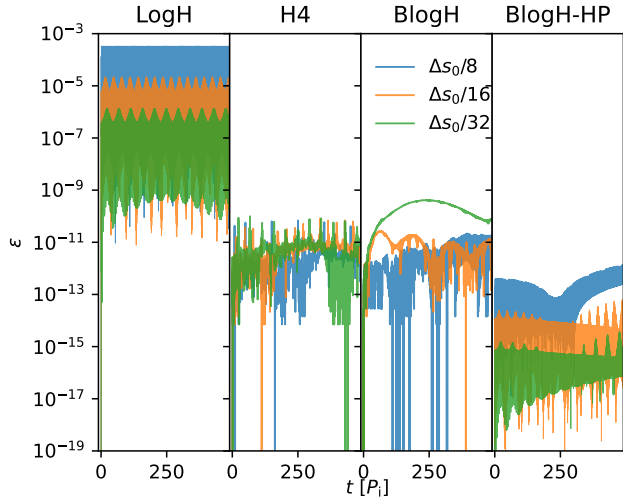


Figure 4. The energy errors ϵ as a function of time are compared for the LogH, H4 BlogH methods, depending on Δs , in simulating the orbital evolution of the triple system with a weakly perturbed binary. The first three panels display the results for each method, while the last panel features the high-precision BlogH method using the 6th-order Yoshida symplectic method with quadruple precision (30 digits) of floating-point numbers.

Comparing the evolution of ϵ reveals a significant advantage for the H4 and BlogH methods. As shown in Figure 4, both methods demonstrate much better energy conservation than the LogH method with the same Δs . In particular, ϵ oscillates significantly in the LogH results, unlike in the other two methods. Compared to Figure 2, the H4 and BlogH methods show a behavior similar to the LogH method for isolated binaries, suggesting that hybrid methods can effectively approximate the Kepler solution for the inner binaries.

A counterintuitive behavior of the BlogH methods is that a smaller Δs leads to a larger ϵ . This occurs because the influence from round-off errors becomes significant and exceeds the approximation error. To investigate this, we performed reference simulations using a high-precision BlogH method (BlogH-HP) which applies quadruple precision with 30 digits. As shown in the last panel of Figure 4, the same Δs results in a lower ϵ , and the relationship between Δs and ϵ aligns with the 2nd-order integration method.

For both BlogH and BlogH-HP results, secular patterns emerge in the evolution of ϵ . To investigate their origin, we further explore how the evolution of orbital parameters from different methods influences the behavior of ϵ . In the triple system with a weakly perturbed

binary, changes in orbital parameters are minimal. To highlight the differences among the methods in the plot, we define the relative evolution of orbital parameters as

$$\Delta o = |o - o[0]| \quad (26)$$

where o represents orbital parameters such as a_i , a_o , e_i and e_o , and $o[0]$ denotes the initial value at $t = 0$.

The results are presented in Figure 5. In addition to the BlogH-HP models, we introduce the BlogH-Y6-HP models, which use both quadruple precision and the Y6 method to enhance integration accuracy. The BlogH-Y6-HP-S256 model is the most accurate simulation and serves as a reference. By comparing the evolution of Δa_i and Δe_i across different methods, we observe that the significant oscillation of ϵ in the LogH models arises from errors in the orbital elements of the inner binary. The LogH models exhibit substantial discrepancies compared to the reference model, with smaller Δs resulting in reduced discrepancies. In contrast, both the H4 and BlogH methods demonstrate comparable inner orbital evolution, aligned closely with the reference model and showing a weak dependence on Δs .

The evolution of outer orbital elements shows that both LogH and BlogH are similar but significantly larger than the reference model. This explains the secular change in ϵ for the BlogH method (Figure 4), which arises from errors in the outer orbital evolution. Furthermore, for the BlogH-S256 model, the ϵ curve in Figure 4 roughly follows the lower boundary of the LogH curve, suggesting that the LogH ϵ curve combines the oscillations of inner binary errors with the secular component from outer binary errors.

In contrast, the H4 method shows improved outer orbital evolution, with smaller Δa_o and Δe_o closely aligned with the reference model. This indicates that the fourth-order H4 method is more accurate for secular evolution of the outer orbit, even though it is not symplectic.

There is no clear trend regarding how the secular patterns of outer orbital evolution appeared in LogH and BlogH results depend on Δs . One possible explanation is that different Δs values lead to varying time phase errors in the inner orbits, resulting in different interactions between the inner and outer orbits and, consequently, different secular patterns.

Although the BlogH method is less accurate in secular evolution compared to the H4 method, it incurs significantly lower computing costs because of the absence of time synchronization. We compare the total number of integration steps, n_s , reflecting these costs for the H4 and BlogH methods in Table 1. The total steps for the H4 method, $n_s(H4, tot)$, are 2-5 times greater

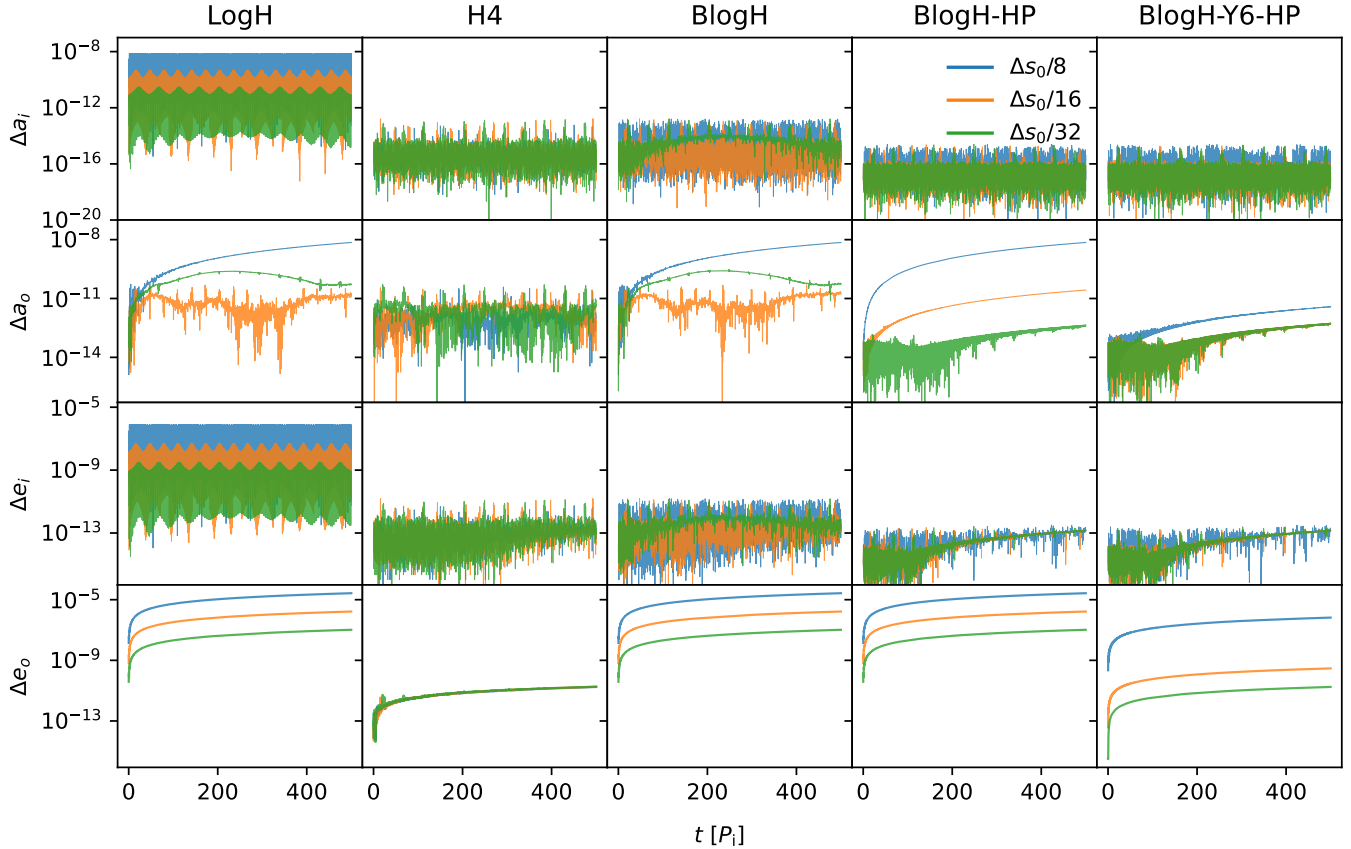


Figure 5. The relative evolution of orbital parameters including semi-major axes and eccentricities of the inner and the outer orbits in the triple including a weakly perturbed binary. The columns represent different methods, while the colors indicate various values of Δs .

Table 1. The step sizes Δs and Δt_H , along with the number of integration steps for the inner binaries in the triple system simulations using the H4 and BlogH methods. The model name suffix indicates the value of Δs . For the H4 method, both the total steps (tot) and the steps for time synchronization are presented. The LogH method has a similar n_s as the BlogH method and is therefore not included.

Model suffix	S16	S64	S256
$\Delta s/\Delta s_0$	1/16	1/64	1/256
$\Delta t_H/P_1$	0.307	0.154	0.077
$n_s(\text{H4,tot})$	42824	89606	227963
$n_s(\text{H4,syn})$	22191	38424	69269
$n_s(\text{BlogH})$	8001	32004	127995

that those for the BlogH method, depending on Δs . The steps for time synchronization, $n_s(\text{H4,syn})$, account for approximately 1/3 – 1/2 of the total steps. This suggests that time synchronization significantly affects the performance of the H4 method.

The values of n_s can indicate the performance of the algorithm; however, the actual wall clock time (t_w) per inner orbit of the simulation can be influenced by various

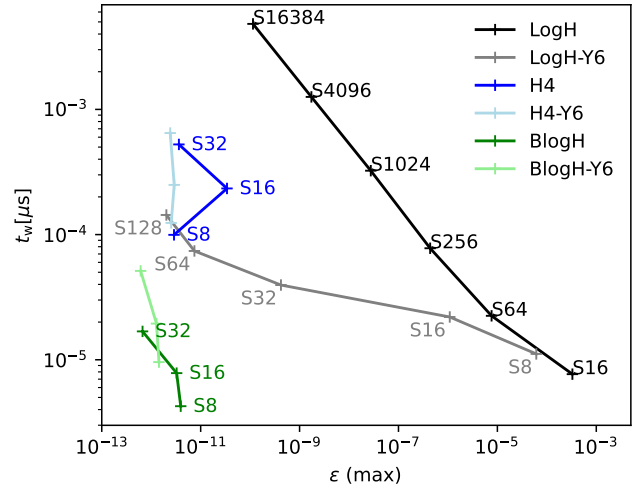


Figure 6. The relationship between maximum ϵ and wall clock time t_w for simulations of the triple system, which includes a weakly perturbed binary. The three methods are compared across different Δs values (indicated on the plot), both with and without the Y6 method.

aspects of implementation. Therefore, we compare the

maximum ϵ within the evolution of 5 P_i versus t_w for the three methods—LogH, H4 and BlogH—across different Δs values, both with and without the Y6 method. The results are shown in Figure 6.

The LogH results show an increasing trend in t_w as both Δs and ϵ decrease. However, the H4 and BlogH methods have ϵ values that are already dominated by round-off errors, so smaller Δs does not significantly reduce ϵ and may even lead to an increase. Therefore, it is preferable to use a larger Δs for the H4 and BlogH methods, such as S8, for better performance.

When only the second-order method is employed, both H4 and BlogH exhibit a few orders of magnitude less t_w compared to the LogH method. However, when the Y6 method is applied, LogH-Y6 becomes comparable to the H4 method at $\epsilon \approx 10^{-11}$. In contrast, the BlogH method still demonstrates at least one order of magnitude less t_w , indicating its significant advantage in computational efficiency.

Please note that the absolute values of t_w for each method can vary depending on the computing hardware and the implementation of the algorithm. The H4 method implemented in the code SDAR is significantly more complex than the LogH or BlogH methods; therefore, although the values of n_s for the H4 method may appear better than those for the LogH method at $\epsilon \approx 10^{-11}$, the actual t_w remains comparable.

4.4. Kozai-Lidov triples

The Hybrid and BLogH methods are accurate not only for triples including a weakly perturbed binary but also significantly enhance accuracy in solving triple systems experiencing Kozai-Lidov oscillations with a highly eccentric inner binary.

When a triple system meets the orbital criterion for Kozai-Lidov oscillation, the inner eccentricity e_i and the inclination angle θ between the inner and outer orbits do oscillate on a timescale given by (e.g. Antognini 2015):

$$t_{\text{KL}} \approx \frac{8}{15\pi} \left(1 + \frac{m_1 + m_2}{m_3} \right) \frac{P_o^2}{P_i} (1 - e_o^2)^{3/2}. \quad (27)$$

In the following example, we set an initial condition for a Kozai-Lidov triple shown in Figure 7. The outer body has $m_3 = 10$, significantly more massive than the inner binary with $m_1 = 0.009$ and $m_2 = 0.001$. The initial inclination θ is 90° and the corresponding t_{KL} is approximately 1138. We can scale the triple to different astrophysical systems. For instance, with a mass unit of $100 M_\odot$, the triple represents a stellar-mass binary of 0.1 and $0.9 M_\odot$ orbiting an intermediate-mass black hole of $1000 M_\odot$. Alternatively, with a mass unit of $0.1 M_\odot$, the triple represents a solar system with binary Jupiter-mass planets.

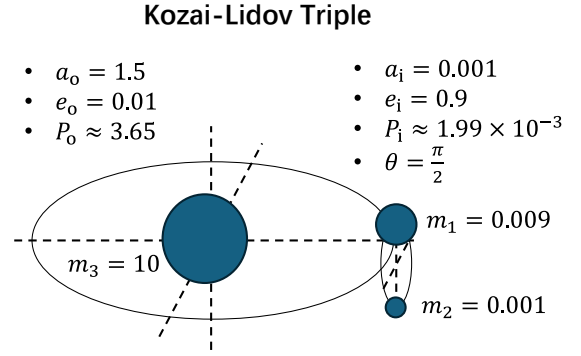


Figure 7. The diagram illustrating the initial condition of the triple where the Kozai-Lidov effect induces high eccentricity in the inner binary.

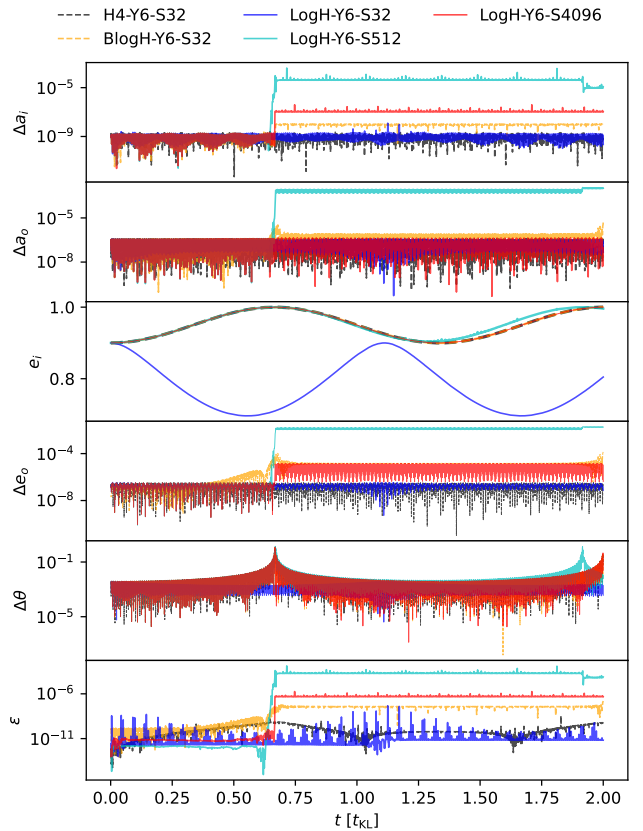


Figure 8. The relative evolution of orbital parameters for the Kozai-Lidov triple. The plotting style is similar to that of Figure 5, with e_i shows as an absolute value instead of Δe_i . The last row displays ϵ .

Using the three methods, we integrate the evolution of the triple for about $2 t_{\text{KL}}$. The orbital parameters and ϵ evolution are shown in Figure 8. We compare the results of all the methods with a step size of $\Delta s = \Delta s_0/32$. The LogH-Y6-S32 model exhibits a markedly different evolution of e_i compared to the H4-Y6-S32 and BlogH-

Y6-S32 models, indicating an unphysical result of the LogH method.

To verify this, we add two simulations using the LogH method with much smaller step sizes: S512 and S4096. These models show a consistent evolution of e_i with H4-Y6-S32 and BlogH-Y6-S32, confirming that LogH-Y6-S32 presents an unphysical result, despite its lower ϵ . Moreover, even with smaller steps, the LogH models display jumps in a_i , e_o and ϵ when e_i approaches unity (approximately 0.9999999). This behavior is less pronounced in the BlogH-Y6-S32 model and absent in the H4-Y6-S32 method, both at the same maximum e_i . This suggests that the LogH method is significantly less accurate than the other two when dealing with high eccentric Kozai-Lidov triples.

We further compare the step counts of the methods in Table 2. The H4-Y6-S32 model has approximately twice as many as the BlogH-Y6-S32 model, suggesting that time synchronization affects the efficiency of the H4 method, consistent with the findings for triples including a weakly perturbed binary in Section 4.3. With the same Δs , the LogH-Y6-S32 model requires about 7.4 times more steps than the BlogH-Y6-S32 model. This indicates that the relationship between Δs and ΔE in Equation 11 for the Kepler orbit is also disrupted in the LogH-Y6-S32 model. The LogH-Y6-S8192 model, which exhibits similar accuracy in orbital evolution to the BlogH-Y6-S32 model, needs around 256 times more steps per orbit. Therefore, the BlogH method demonstrates a significant performance advantage.

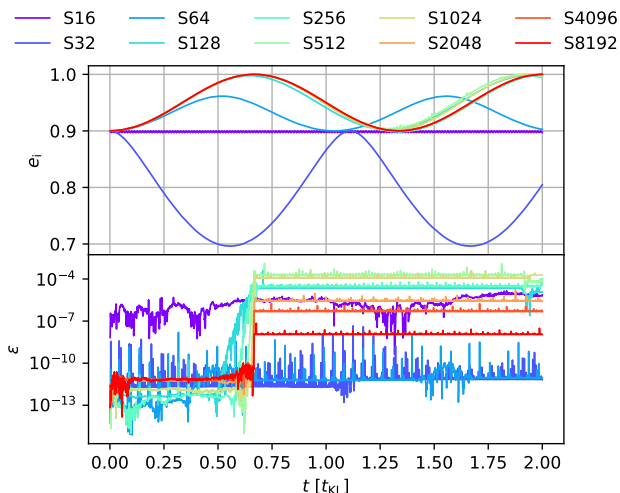


Figure 9. The evolution of e_i and ϵ in the simulations of the Kozai-Lidov triple using the LogH method with varying Δs .

Two major issues with the low accuracy of the LogH method are the unphysical evolution of e_i and the sig-

nificant jump in ϵ when e_i is close to 1. To investigate how these behaviors depend on Δs , we perform a series of models using the LogH method with varying Δs . The evolutions of e_i and ϵ are compared in Figure 9.

The S16, S32 and S64 models show significantly different secular evolutions of e_i . In these simulations, the n_s per P_i are 135, 269 and 538, respectively. Despite using the high-accuracy 6th-order Yoshida method, e_i still evolves unphysically. In addition, repeated peaks appear in the evolution of ϵ for the S32 and S64 models. These peaks occur at the periapsis of the inner binary, as illustrated by the LogH results for the triple, including a weakly perturbed binary (Figure 2). This suggests that the low accuracy at periapsis from the LogH method introduces an artificial perturbation that repeatedly impacts e_i and leads to an unphysical secular evolution.

Despite the unphysical evolution of e_i , ϵ can still recover to a low value, aligned with the symplectic method. The maximum ϵ reaches approximately 10^{-8} , corresponding to a relative energy error of 10^{-6} . Although this relative error may be acceptable for N -body simulations of star clusters, it is insufficient for this triple system. We also investigated whether the artificial perturbation originates from backward steps in the 6th-order Yoshida method and found no correlation.

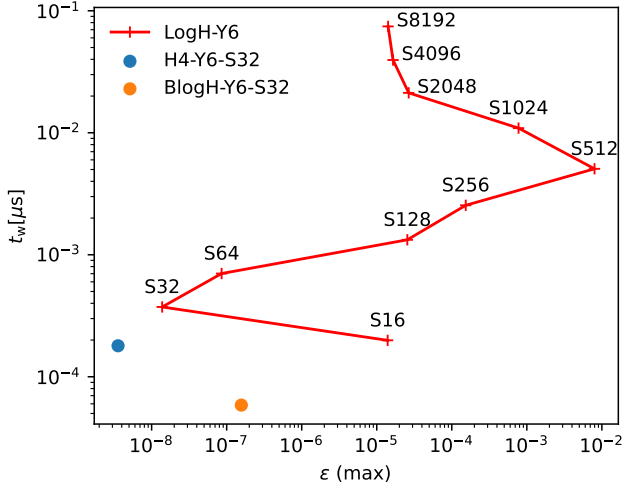
As Δs increases from S128 to S8192, the evolution trend of e_i converges with the H4 and BlogH results, and jumps in ϵ begin to appear. While the jump value decreases, the average value of ϵ increases as Δs decreases. This suggests that a smaller Δs can help minimize a large jump but increases cumulative round-off errors. This inverse relationship between Δs and the average ϵ also occurs in the simulations for the triple including a weakly perturbed binary, as illustrated in Figure 4.

An important feature is that the S32 and S64 models show a similar average ϵ . Because e_i is far from 1, there is no jump in ϵ . In contrast, for the S128 models, the jump occurs at $e_i \approx 1$, resulting in a final ϵ that is significantly larger than those of the S32 and S64 models. If we rely solely on the final ϵ to assess integration accuracy without considering the secular evolution of e_i , we may mistakenly conclude that the S32 and S64 models are more accurate.

We now compare the maximum ϵ and t_w for the LogH-Y6 models with different Δs values, as well as for the BlogH-Y6-S32 and H4-Y6-S32 models. The results are presented in Figure 10. For the LogH-Y6 method, below S256, the evolution of e_i is unphysical; consequently, ϵ appears low and increases with Δs , along with t_w , except for S16. Above S512, energy jumps when e_i approaches 1 dominate the maximum ϵ , leading to a more reasonable

Table 2. Step counts (n_s) for different methods used to integrate the Kozai-Lidov triple. Both total n_s and n_s per P_1 are shown.

Model name	BlogH-Y6-S32	H4-Y6-S32	LogH-Y6-S32	LogH-Y6-S4096	LogH-Y6-S8192
n_s	3.5e+07	6.9e+07	2.9e+08	3.7e+10	7.5e+10
n_s [per P_1]	32	64	269	34437	68874

**Figure 10.** The relationship between maximum ϵ and wall clock time t_w for simulations of the Kozai-Lidov triple system. The plotting style is similar to that of Figure 6.

trend where increasing Δs leads to a lower maximum ϵ . Comparing this with Figure 6, we observe that the H4 and BlogH methods demonstrate greater efficiency at equivalent ϵ values when solving the Kozai-Lidov triples with high eccentricities, and the H4 method being notably more efficient than the LogH method.

Note that for the LogH method, the maximum ϵ is primarily attributed to the energy jumps. It is also possible to reduce the step sizes when e_i is close to 1 to avoid significant energy jumps, although this breaks the simplicity of the (original) LogH method. Consequently, with larger Δs values, such as S512, it becomes feasible to obtain a reasonable physical result with much lower maximum ϵ .

5. CRITERION FOR SWITCHING BETWEEN LOGH AND BLOGH METHODS

The H4 and BlogH methods demonstrate significantly better accuracy than the LogH method for hierarchical triples; however, they lack generality. As perturbation on the inner binary increases, its motion diverges more from the Kepler orbit, reducing the advantage of the hybrid methods while enhancing the LogH method's performance. In cases of unstable or chaotic triples where the inner binary cannot be clearly defined, the LogH method is expected to outperform the hybrid methods.

Since the perturbation on the inner binary depends on m_3 and the separation between the third body and

the inner binary, we perform a large set of simulations by varying the initial m_3 and a_o of based on the initial condition of the Kozai-Lidov triple. We select 20 values for m_3 ranging from 1 to 10 and 20 values for a_o from 0.01 and 0.1 on a logarithmic scale, generating a total of 20×20 initial conditions from each pair. For each initial condition, we perform four simulations using the LogH and BlogH methods with two values of Δs : S32 and S256. The H4 method is excluded due to its similar performance to the BlogH method.

The secular evolution of e_i in the Kozai-Lidov triple serves as a good indicator to identify the most suitable method. Figure 11 displays three typical simulations that illustrate the points at which the LogH and BlogH methods change behavior. In the left panel, with $m_3 = 10$ and $a_i = 0.01$, e_i evolve above 1.0, indicating a binary disruption event caused by strong tidal forces from the third object. The LogH results with S32 and S256 show a consistent evolution of e_i and produce significantly lower values of ϵ compared to the BlogH results. Therefore, the LogH method is superior to the BlogH method.

In contrast, the BlogH method outperforms the LogH method in the right panel with $a_i = 0.1$. The Kozai-Lidov oscillation of e_i with sub-oscillation is observable. The LogH-S32 method provides a nonphysical evolution, while the BlogH method exhibits a consistent evolution of e_i . The BlogH-S256 result yields better ϵ than the LogH-S32 result.

The middle panel illustrates the transition case, where both methods behave similarly. The e_i shows an irregular evolution but remains undisturbed by strong perturbations from the third object. The S256 results for both methods exhibit similar ϵ values. The LogH-S32 model has a smaller ϵ than the BlogH-S32 model before $\sim 1.6t_{\text{KL}}$, but it surpasses it after a jump.

To establish the quantitative condition for determining the best method, we define δe_i as the absolute difference in e_i at $t = 2t_{\text{KL}}$ between the S16 and S256 results. A small δe_i indicates convergence to a similar final e_i , while a large value suggests non-convergence and unphysical behavior. We then define the ratio of δe_i between the two methods as

$$\mathcal{R}_e = \frac{\delta e_i [\text{LogH}]}{\delta e_i [\text{BlogH}]} \quad (28)$$

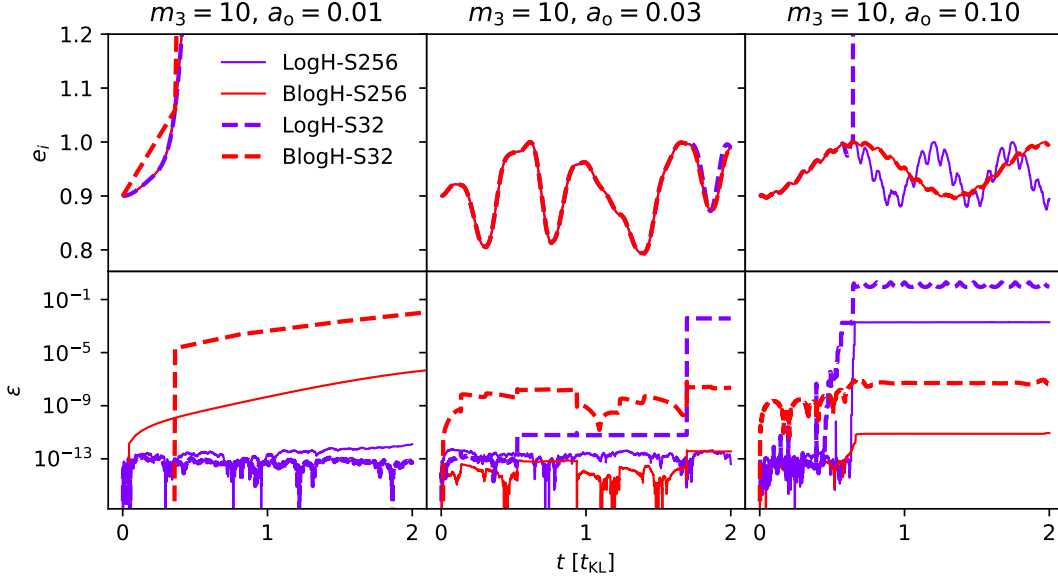


Figure 11. The evolution of e_i and ϵ for three typical simulations of the Kozai-Lidov triple, each with varying a_o values. From left to right, the e_i evolution shows binary disruption, irregular evolution, and regular oscillation. The LogH and BlogH methods are represented in different colors, while different line types indicate the various Δs .

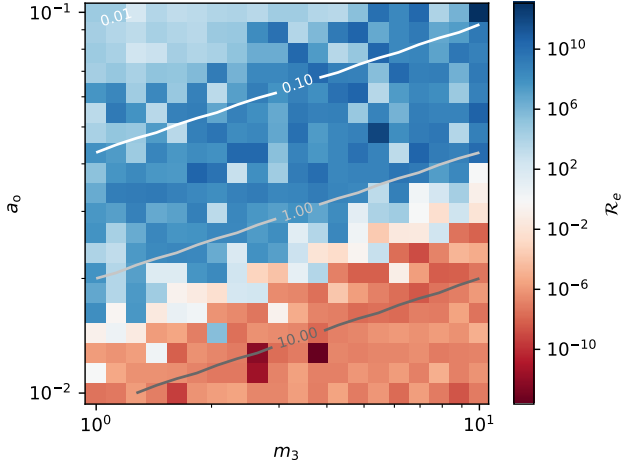


Figure 12. The color map displaying the ratio of δe_i between the LogH and BlogH results, denoted as \mathcal{R}_e , where δe_i represents the difference in e_i between S16 and S256 at $2t_{\text{KL}}$. The contour illustrates the perturbation ratio \mathcal{R}_p of the outer and inner orbits.

When $\mathcal{R}_e > 1$, the BlogH method shows better convergence in the secular evolution of e_i and is therefore preferred. Consequently, the curve where $\mathcal{R}_e = 1$ indicates the switching condition.

Figure 12 displays the color map of \mathcal{R}_e , showing a clear gradient related to both m_3 and a_o . This gradient trend is well-explained by the tidal perturbation from the third body on the inner binary. We define the ratio between the outer perturbation and the inner binary's

force as follows:

$$\mathcal{R}_p = \frac{m_3 (m_1 + m_2)}{m_1 m_2} \left[\frac{a_i (1 + e_i)}{a_o (1 - e_o)} \right]^3, \quad (29)$$

which reflects the maximum ratio at the apoapsis of the outer orbit and the periapsis of the inner orbit. The contour of \mathcal{R}_p in Figure 12 can be described by $\mathcal{R}_p = C$, where C is a constant. The curve of $\mathcal{R}_e = 1$ lies within the range of C from 1 to 10. Thus, we can use the simple switching criterion of $\mathcal{R}_p > 1$ to use the LogH method instead of the BlogH for triple systems.

This switching criterion is derived for the Kozai-Lidov triple and may not be suitable for all triple systems. When the outer orbit is highly eccentric or hyperbolic, the perturbation on the inner binary varies significantly, making this criterion less effective. We may need a more reliable switching condition based on the separation between the third body and the inner binary. However, such a criterion could lead to frequent switching as the third body approaches and departs from periapsis. In future work, a thorough investigation is required to design a more general switching criterion, possibly incorporating the method suggested by (Hernandez & Dehnen 2023) to reduce cumulative switching errors.

6. DISCUSSION

6.1. Limitations of the BlogH method

The absence of time synchronization offers advantages to the BlogH method, but also limits its applicability. When two binaries exist in a system, such as a binary-binary quadruple, the LogH method must be applied

to each binary with different time transformation functions. In this case, the same Δs results in different Δt values for the two binaries, making time synchronization unavoidable and preventing the use of the BlogH method. In future studies, we will explore the extension of the BlogH approach to systems with multiple binaries.

6.2. Combination with the Bulirsch-Stoer method

To address the low accuracy of the second order sDKD method in the LogH approach (for both original and MA2002 methods), Mikkola & Tanikawa (1999) applied the Bulirsch-Stoer extrapolation integrator to create the LogH-BS method. This method uses polynomial extrapolation on a sequence of LogH results obtained through the sDKD loop with varying step sizes of Δs , predicting an accurate result as the step size approaches zero.

The Bulirsch-Stoer method is efficient when paired with a classic integrator. However, the LogH-BS method is less efficient than the pure LogH method for binary systems. The LogH method can precisely follow the trajectory of a Kepler orbit with only a time-phase error, whereas the extrapolated results from the LogH-BS method do not guarantee exact alignment with the trajectory. To achieve the same accuracy as the LogH method, the LogH-BS method requires more integration steps.

The LogH-BS method is more beneficial for systems with $N > 2$. However, as illustrated in Figure 9, for Kozai-Lidov triples, a low ϵ does not ensure accurate secular evolution of e_i . Therefore, only with a strict criterion of $\epsilon < 10^{-11}$, can the LogH-BS method potentially provide a physical evolution of e_i while avoiding large errors at the periastron of the inner binary. In contrast, hybrid methods such as the H4 or BlogH method are much more efficient.

The hybrid methods can be combined with the Bulirsch-Stoer method for faster convergence of hierarchical triples. Further investigation of this possibility is needed in future work.

6.3. Time Phase Error

For all three methods, the time phase has errors due to the approximation in time integration, which manifests itself as an artificial phase shift when a large Δs is used. This error also affects time synchronization in the H4 method. Depending on the systems being studied, this error can be significant or negligible. In planetary systems where orbital resonances are important, such phase errors may impact long-term evolution and should be carefully investigated. However, for multiple systems in star clusters, which is the focus of this

work, the error in the time phase is less critical than the errors in energy and angular momentum. This is because studies of star clusters primarily concentrate on the statistical evolution of semi-major axes and eccentricities of binaries, which are essential for estimating merger rates and orbital properties of events like gravitational waves. Thus, the orbital (time) phase is not important. Consequently, orbital average methods that may produce incorrect time phases, such as the slow-down method (Mikkola & Aarseth 1996; Wang et al. 2020b), are frequently employed in star cluster simulations to enhance efficiency, including codes like NBODY6, PETAR and BIRFOST. More research is needed to explore how orbital average methods can be integrated with the hybrid method.

7. SUMMARY

In this work, we demonstrate that the LogH method (algorithmic regularization) effectively traces Keplerian trajectories in binary systems, but is significantly less accurate for multiple systems like triples. As shown in Figure 2, even adding a third body with weak perturbation to a binary can introduce significant errors, causing the LogH method to lose the ability to trace Keplerian trajectories and revert to a standard second-order symplectic method. Furthermore, the LogH method can lead to an unphysical secular evolution of e_i in a Kozai-Lidov triple, as shown in Figure 8, unless the step size is extremely small. We also found that the energy error, a traditional indicator of integration quality, may fail to identify the unphysical secular evolution of e_i in the Kozai-Lidov triple.

For hierarchical triples, a more effective solution is to use hybrid methods that combine two integrators, using the LogH method only for the inner binary. One commonly used hybrid method is H4 (Hermite + LogH), which offers significantly improved accuracy with a step size similar to that of the LogH method; however, it requires time synchronization, adding additional cost.

In this work, we introduce a new hybrid method, BlogH, which combines the LogH method for the inner binary and a sDKD method for outer bodies, using the same time steps. The BlogH method not only achieves a similar accuracy as H4, but is also more efficient without the need for time synchronization. Its implementation is straightforward, requiring only modifications to the time transformation function of the LogH method. The preliminary implementation of the BlogH method is available in the experimental branch of the SDAR code (version 329e).

The main drawback of BlogH is that it is applicable only to multiple systems with one inner binary. In fu-

ture work, we will explore a new hybrid algorithm without time synchronization as an extension of the BlogH method for more general N -body systems with multiple inner binaries.

Additionally, the BlogH method becomes less accurate than the LogH method when the inner binary is strongly perturbed. We can establish a switching criterion to select the optimal method based on the integrated N body system. We find that Equation 29 serves as a reasonable criterion for this purpose. In future studies, we will test a wider range of initial conditions for triples to validate and improve the switching criterion.

8. ACKNOWLEDGMENTS

We thank the very useful comments from the referee. We thank the support of the National Natural Science Foundation of China through grants 21BAA00619 and 12233013, the one-hundred-talent project of Sun Yat-sen University, the Fundamental Research Funds for the Central Universities, Sun Yat-sen University (22hytd09).

Software: numpy (Harris et al. 2020), matplotlib (Hunter 2007), SDAR (Wang et al. 2020b, GitHub: <https://github.com/lwang-astro/SDAR>)

APPENDIX

A. COMPARISON OF THE ORIGINAL LOGH AND MA2002 METHODS

A.1. Binaries

Although the original LogH method can trace the Keplerian trajectory with approximation errors affecting only the time phase, as shown by Preto & Tremaine (1999) and Wang & Nitadori (2020), ϵ does not reach the round-off error limit of the floating-point precision. This occurs because the symplectic map in the LogH method solves the equation of motion using the extended Hamiltonian $\Gamma = \log(T(\mathbf{P})) - \log(-U(\mathbf{R})) = \log(T(\mathbf{P})/ -U(\mathbf{R}))$. Thus, it conserves Γ or $T(\mathbf{P})/U(\mathbf{R})$ instead of the original Hamiltonian H or energy, as shown in Equation 43, 44a and 45a of Preto & Tremaine (1999). We can approximate $g(\mathbf{W})$ as $f'(-U)$, following Equation 26 in Preto & Tremaine (1999). Thus, for the LogH method, we have:

$$\Gamma \approx \frac{1}{-U}[H + p_t]. \quad (\text{A1})$$

The absolute energy error, $\epsilon = |H + p_t|$, can be approximated by $|-U\Gamma|$. For an eccentric binary, $-U$ reaches its maximum value at periapsis. Therefore, although the method ensures that Γ is only affected by round-off errors, the error can be significantly amplified by $-U$ when converted to ϵ . Furthermore, if the separation between the two binary components changes significantly in one step, round-off errors can also significantly affect Γ , preventing it from reaching the round-off error limit.

To illustrate this behavior, we evolve an extremely eccentric binary with $1 - e = 1 \times 10^{-8}$ and other initial orbital parameters based on the setup in Figure 1. Such an extreme case can amplify errors. The evolutions of ϵ , original $|\Gamma|$, and approximated $|\Gamma|$ (A1) from Equation A1 for the original LogH and MA2002 methods are shown in Figure 13. The upper panels display results with double-precision floating points, while the lower panel shows results with 30-digit precision. In both cases, $|\Gamma|$ is two orders of magnitude smaller than ϵ . Based on the orbital parameters, $-U$ is of the order of 10^2 at apoapsis, consistent with the offset between Γ and ϵ . The results also indicate that $|\Gamma|$ (A1) nearly overlaps with $|\Gamma|$, confirming it as a good approximation.

At periapsis, ϵ exhibits a significant peak due to round-off errors, which is absent in Γ for the original LogH method and even decreases for the MA2002 method. With $-U$ on the order of 10^{10} at periapsis, we expect the maximum value of ϵ to reach 10^{-4} at the exact periapsis for double precision results. However, since the simulations do not precisely reach periapsis, the maximum value is significantly lower.

We observe that the MA2002 method is less accurate than the original LogH method due to the approximation of u . This approximation also leads to a distinct pattern in $|\Gamma|$ from periapsis to apoapsis. Despite its lower accuracy, the method can still approximate the Keplerian trajectory, significantly outperforming the classical symplectic LeapFrog method for extremely high eccentric binaries.

As the precision increases from double to 30-digit, the magnitude of γ decreases by an order of 14 for both methods, indicating that the error in Γ is mainly due to round-off errors. If the approximation errors were dominant, we would not expect such a significant decrease, as the approximation errors depend mainly on Δs , which remains unchanged.

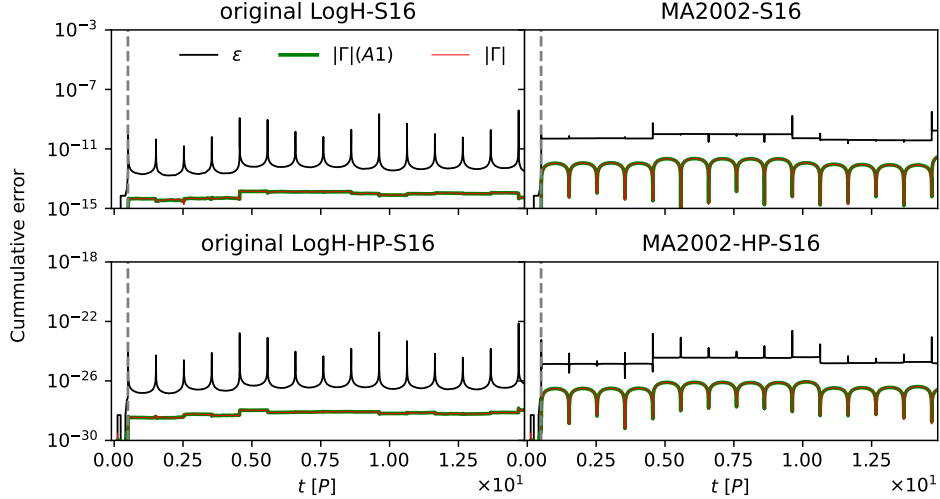


Figure 13. Cumulative absolute integration errors for an extremely eccentric binary ($1 - e = 1 \times 10^{-8}$) using the original LogH and MA2002 methods. The absolute energy errors (ϵ), the absolute extended Hamiltonian ($|\Gamma|$) and the approximated $|\Gamma|$ from Equation A1 are compared. The upper and lower panels show simulations with double precision and 30-digit precision, respectively. The vertical dashed line marks the first periapsis passage.

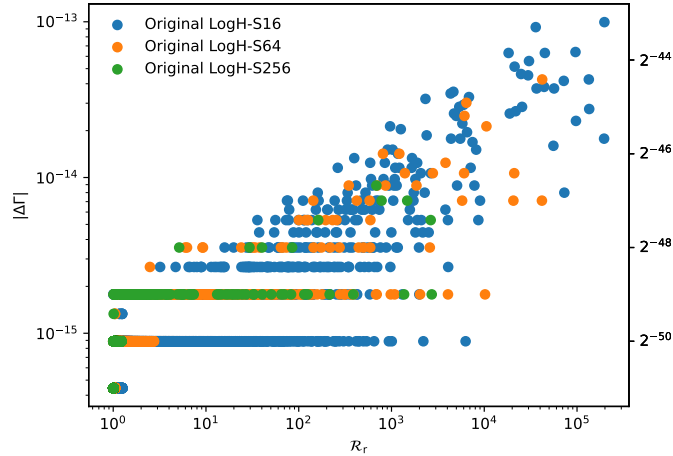


Figure 14. The change in Γ during a single integration step relative to the ratio of the distances between the binary components before and after integration (the ratio of the maximum to the minimum distance). Simulations of the highly eccentric binary using the original LogH methods with varying Δs are compared.

In Figure 13, jumps in Γ occur when the orbit approaches periapsis, probably also due to round-off errors. As the orbit passes periapsis, the change in distances between the binary components (r) can be significant. According to one drift step of Equation 8, if the new r is 10^n times smaller than the previous r , the drift calculation introduces n digits of round-off errors. These errors can ultimately affect Γ and may not be recoverable.

To illustrate this, we investigate how the jumps in Γ depend on changes in r for simulations of the extremely high eccentricity binary using the original LogH method with varying Δs . We define \mathcal{R}_r as the ratio of r before and after the step (the ratio of the maximum to the minimum r). Figure 14 shows the relationship between $|\Delta\Gamma|$, the change in $|\Gamma|$ in one step, and \mathcal{R}_r .

The results indicate a correlation between $|\Delta\Gamma|$ and \mathcal{R}_r . For a given value of \mathcal{R}_r , $\Delta\Gamma$ exhibits a wide range of variations, indicating that the correlation between the two is not strict. This is consistent with the expectation that $\Delta\Gamma$ arise from round-off errors: Since the rounding errors from changes in r are random, $\Delta\Gamma$ does not always experience large jumps, but rather they occur sporadically.

When $\Delta\Gamma$ is below 10^{-14} , the values appear in discrete sequences due to the conversion from binary to decimal. The right y -axis in Figure 14 displays $\Delta\Gamma$ values on a logarithmic scale with base 2, where the power index represents individual bits in computer memory. This reveals that these discrete sequences correspond to each bit. For double precision, the minimum representable value is 2^{-52} , which corresponds to approximately 2.22×10^{-16} . This suggests that the discrete $\Delta\Gamma$ values reflect the limitations of double precision, indicating that they are influenced by the last few bits of precision.

The correlation (upper boundary) between $|\Delta\Gamma|$ and \mathcal{R}_r is independent of Δs , indicating that $|\Delta\Gamma|$ is unlikely due to approximation errors related to Δs and is instead directly related to \mathcal{R}_r . However, when Δs is small, the likelihood of achieving a large \mathcal{R}_r decreases, leading to a smaller maximum $|\Delta\Gamma|$. This suggests that reducing Δs may help minimize maximum Γ errors, but this effect is only seen in the original LogH method. In the following analysis, the MA2002 method shows an opposite trend.

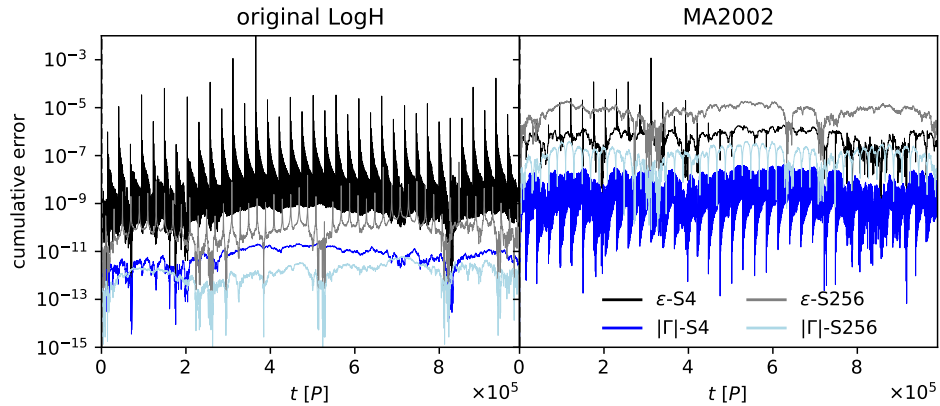


Figure 15. Cumulative absolute integration errors for the extremely eccentric binary ($1 - e = 1 \times 10^{-8}$) are compared using the original LogH and MA2002 methods, with time integrated over 10^6 periods and two values of Δs , S4 and S256.

To investigate the long-term behavior of the two methods, we continue to integrate the binary over 10^6 periods, the cumulative errors are shown in Figure 15. For the original LogH method, the two values of Δs , S4 and S256, result in similar level of Γ and ϵ . The maximum value of errors are lower with S256, due to less maximum \mathcal{R}_r .

In contrast, the MA2002 method exhibits an interesting behavior: smaller Δs leads to larger errors. This may be due to smaller Δs introducing more cumulative round-off and approximation errors, causing the results to deviate further from the original method.

Although the MA2002 method is not symplectic, it demonstrates time-symmetric behavior during long-term evolution, as there is no significant drift in errors over 10^6 periods.

A.2. Triples

The behaviors of the two methods for triples, including a weakly perturbed binary discussed in Section 3, are similar. Figure 16 compares ϵ and Γ for the triple using both methods with $\Delta s_0/256$. Both methods yield identical results.

Furthermore, we compare the evolution of another triple system by changing $1 - e_i$ to 1×10^{-8} , as shown in Figure 17. Unlike the isolated binary case in Figure 13, the errors of both ϵ and Γ increase significantly after the first periapsis and do not return. Both methods again yield identical results. The round-off error differences observed in the binary case are diminished by the approximation error in the two triple cases. Therefore, in this work, we only present the MA2002 results, which sufficiently represent the behavior of both methods for triples.

REFERENCES

- Aarseth, S. J. 2003, Gravitational N-Body Simulations
—, 2012, MNRAS, 422, 841,
doi: 10.1111/j.1365-2966.2012.20666.x
- Alessandrini, E., Lanzoni, B., Ferraro, F. R., Mocchi, P., &
Vesperini, E. 2016, ApJ, 833, 252,
doi: 10.3847/1538-4357/833/2/252

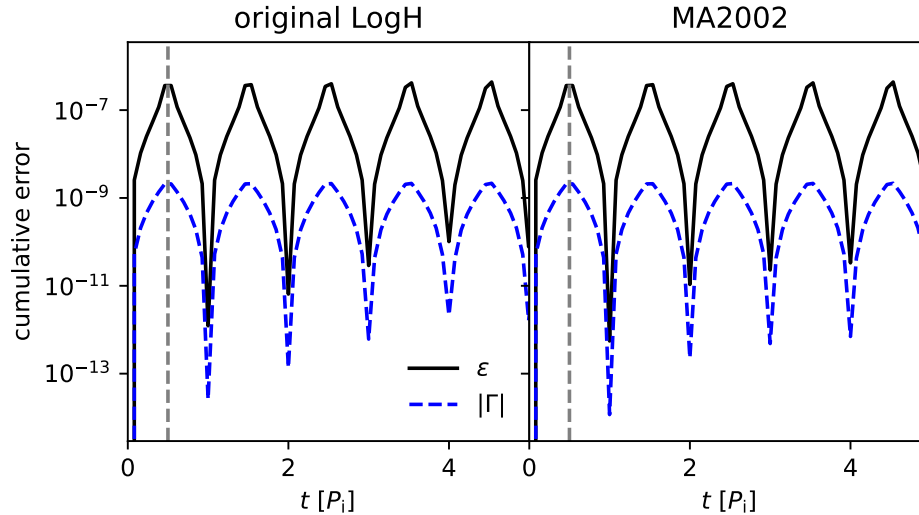


Figure 16. Cumulative absolute integration errors for the same triple, including a weakly perturbed binary, as shown in Figure 2, using the original LogH and MA2002 methods with $\Delta s_0/256$. The plotting style is similar to Figure 13.

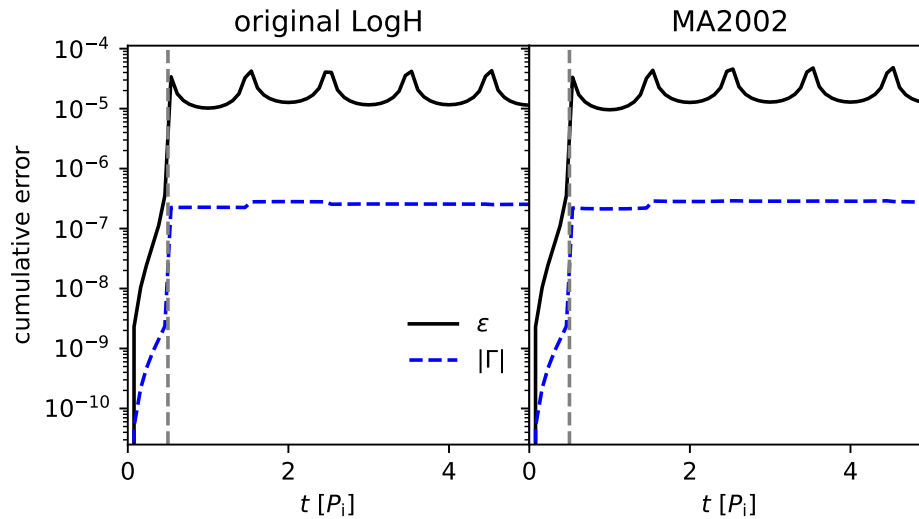


Figure 17. Cumulative absolute integration errors for triples, similar to Figure 16, but with the inner binary eccentricity set to $1 - e = 1 \times 10^{-8}$.

Antognini, J. M. O. 2015, MNRAS, 452, 3610,
doi: [10.1093/mnras/stv1552](https://doi.org/10.1093/mnras/stv1552)

Antonini, F., Chatterjee, S., Rodriguez, C. L., et al. 2016,
ApJ, 816, 65, doi: [10.3847/0004-637X/816/2/65](https://doi.org/10.3847/0004-637X/816/2/65)

Antonini, F., & Gieles, M. 2020, MNRAS, 492, 2936,
doi: [10.1093/mnras/stz3584](https://doi.org/10.1093/mnras/stz3584)

Antonini, F., Murray, N., & Mikkola, S. 2014, ApJ, 781, 45,
doi: [10.1088/0004-637X/781/1/45](https://doi.org/10.1088/0004-637X/781/1/45)

Antonini, F., Toonen, S., & Hamers, A. S. 2017, ApJ, 841,
77, doi: [10.3847/1538-4357/aa6f5e](https://doi.org/10.3847/1538-4357/aa6f5e)

Askar, A., Szkudlarek, M., Gondek-Rosińska, D., Giersz,
M., & Bulik, T. 2017, MNRAS, 464, L36,
doi: [10.1093/mnras/slwl77](https://doi.org/10.1093/mnras/slwl77)

Bae, Y.-B., Kim, C., & Lee, H. M. 2014, MNRAS, 440,
2714, doi: [10.1093/mnras/stu381](https://doi.org/10.1093/mnras/stu381)

Bailyn, C. D. 1995, ARA&A, 33, 133,
doi: [10.1146/annurev.aa.33.090195.001025](https://doi.org/10.1146/annurev.aa.33.090195.001025)

Banerjee, S. 2017, MNRAS, 467, 524,
doi: [10.1093/mnras/stw3392](https://doi.org/10.1093/mnras/stw3392)

—. 2018, MNRAS, 473, 909, doi: [10.1093/mnras/stx2347](https://doi.org/10.1093/mnras/stx2347)

—. 2020, PhRvD, 102, 103002,
doi: [10.1103/PhysRevD.102.103002](https://doi.org/10.1103/PhysRevD.102.103002)

—. 2021, MNRAS, 503, 3371, doi: [10.1093/mnras/stab591](https://doi.org/10.1093/mnras/stab591)

Banerjee, S., Baumgardt, H., & Kroupa, P. 2010, MNRAS,
402, 371, doi: [10.1111/j.1365-2966.2009.15880.x](https://doi.org/10.1111/j.1365-2966.2009.15880.x)

- Chambers, J. E. 1999, *MNRAS*, 304, 793, doi: [10.1046/j.1365-8711.1999.02379.x](https://doi.org/10.1046/j.1365-8711.1999.02379.x)
- Chatterjee, S., Rasio, F. A., Sills, A., & Glebbeek, E. 2013, *ApJ*, 777, 106, doi: [10.1088/0004-637X/777/2/106](https://doi.org/10.1088/0004-637X/777/2/106)
- Chatterjee, S., Rodriguez, C. L., & Rasio, F. A. 2017, *ApJ*, 834, 68, doi: [10.3847/1538-4357/834/1/68](https://doi.org/10.3847/1538-4357/834/1/68)
- Di Carlo, U. N., Giacobbo, N., Mapelli, M., et al. 2019, *MNRAS*, 487, 2947, doi: [10.1093/mnras/stz1453](https://doi.org/10.1093/mnras/stz1453)
- Donada, J., Anders, F., Jordi, C., et al. 2023, *A&A*, 675, A89, doi: [10.1051/0004-6361/202245219](https://doi.org/10.1051/0004-6361/202245219)
- Downing, J. M. B., Benacquista, M. J., Giersz, M., & Spurzem, R. 2010, *MNRAS*, 407, 1946, doi: [10.1111/j.1365-2966.2010.17040.x](https://doi.org/10.1111/j.1365-2966.2010.17040.x)
- Duchêne, G., & Kraus, A. 2013, *ARA&A*, 51, 269, doi: [10.1146/annurev-astro-081710-102602](https://doi.org/10.1146/annurev-astro-081710-102602)
- Eggleton, P. P., & Kiseleva-Eggleton, L. 2001, *ApJ*, 562, 1012, doi: [10.1086/323843](https://doi.org/10.1086/323843)
- Fabrycky, D., & Tremaine, S. 2007, *ApJ*, 669, 1298, doi: [10.1086/521702](https://doi.org/10.1086/521702)
- Fernández, J. J., & Kobayashi, S. 2019, *MNRAS*, 487, 1200, doi: [10.1093/mnras/stz1353](https://doi.org/10.1093/mnras/stz1353)
- Ford, E. B., Kozinsky, B., & Rasio, F. A. 2000, *ApJ*, 535, 385, doi: [10.1086/308815](https://doi.org/10.1086/308815)
- Fragione, G., & Antonini, F. 2019, *MNRAS*, 488, 728, doi: [10.1093/mnras/stz1723](https://doi.org/10.1093/mnras/stz1723)
- Fragione, G., & Loeb, A. 2019, *MNRAS*, 486, 4443, doi: [10.1093/mnras/stz1131](https://doi.org/10.1093/mnras/stz1131)
- Fujii, M. S., Tanikawa, A., & Makino, J. 2017, *PASJ*, 69, 94, doi: [10.1093/pasj/psx108](https://doi.org/10.1093/pasj/psx108)
- Gaia Collaboration, Arenou, F., Babusiaux, C., et al. 2023, *A&A*, 674, A34, doi: [10.1051/0004-6361/202243782](https://doi.org/10.1051/0004-6361/202243782)
- Gonçalves Ferrari, G., Boekholt, T., & Portegies Zwart, S. F. 2014, *MNRAS*, 440, 719, doi: [10.1093/mnras/stu282](https://doi.org/10.1093/mnras/stu282)
- Hairer, E. 1997, *Applied Numerical Mathematics*, 25, 219, doi: [10.1016/S0168-9274\(97\)00061-5](https://doi.org/10.1016/S0168-9274(97)00061-5)
- Hamers, A. S. 2018, *MNRAS*, 476, 4139, doi: [10.1093/mnras/sty428](https://doi.org/10.1093/mnras/sty428)
- . 2020, *MNRAS*, 494, 5492, doi: [10.1093/mnras/staa1084](https://doi.org/10.1093/mnras/staa1084)
- Hamers, A. S., Perets, H. B., Antonini, F., & Portegies Zwart, S. F. 2015, *MNRAS*, 449, 4221, doi: [10.1093/mnras/stv452](https://doi.org/10.1093/mnras/stv452)
- Hamers, A. S., & Portegies Zwart, S. F. 2016, *MNRAS*, 459, 2827, doi: [10.1093/mnras/stw784](https://doi.org/10.1093/mnras/stw784)
- Harris, C. R., Millman, K. J., van der Walt, S. J., et al. 2020, *Nature*, 585, 357, doi: [10.1038/s41586-020-2649-2](https://doi.org/10.1038/s41586-020-2649-2)
- Heggie, D. C. 1975, *MNRAS*, 173, 729, doi: [10.1093/mnras/173.3.729](https://doi.org/10.1093/mnras/173.3.729)
- Heggie, D. C., Trenti, M., & Hut, P. 2006, *MNRAS*, 368, 677, doi: [10.1111/j.1365-2966.2006.10122.x](https://doi.org/10.1111/j.1365-2966.2006.10122.x)
- Hénon, M. 1961, *Annales d'Astrophysique*, 24, 369
- Hernandez, D. M., & Bertschinger, E. 2015, *MNRAS*, 452, 1934, doi: [10.1093/mnras/stv1439](https://doi.org/10.1093/mnras/stv1439)
- Hernandez, D. M., & Dehnen, W. 2023, *MNRAS*, 522, 4639, doi: [10.1093/mnras/stad657](https://doi.org/10.1093/mnras/stad657)
- Hills, J. G. 1975, *AJ*, 80, 809, doi: [10.1086/111815](https://doi.org/10.1086/111815)
- Hong, J., Askar, A., Giersz, M., Hypki, A., & Yoon, S.-J. 2020, *MNRAS*, 498, 4287, doi: [10.1093/mnras/staa2677](https://doi.org/10.1093/mnras/staa2677)
- Hunter, J. D. 2007, *Computing in Science & Engineering*, 9, 90, doi: [10.1109/MCSE.2007.55](https://doi.org/10.1109/MCSE.2007.55)
- Hurley, J. R., Tout, C. A., Aarseth, S. J., & Pols, O. R. 2001, *MNRAS*, 323, 630, doi: [10.1046/j.1365-8711.2001.04220.x](https://doi.org/10.1046/j.1365-8711.2001.04220.x)
- Hypki, A., & Giersz, M. 2013, *MNRAS*, 429, 1221, doi: [10.1093/mnras/sts415](https://doi.org/10.1093/mnras/sts415)
- Kremer, K., Rodriguez, C. L., Amaro-Seoane, P., et al. 2019, *PhRvD*, 99, 063003, doi: [10.1103/PhysRevD.99.063003](https://doi.org/10.1103/PhysRevD.99.063003)
- Kroupa, P. 1995, *MNRAS*, 277, 1491, doi: [10.1093/mnras/277.4.1491](https://doi.org/10.1093/mnras/277.4.1491)
- Kumamoto, J., Fujii, M. S., & Tanikawa, A. 2019, *MNRAS*, 486, 3942, doi: [10.1093/mnras/stz1068](https://doi.org/10.1093/mnras/stz1068)
- Kustaanheimo, P., & STIEFEL, E. 1965, *Journal für die reine und angewandte Mathematik (Crelles Journal)*, 1965, 204, doi: [10.1515/crll.1965.218.204](https://doi.org/10.1515/crll.1965.218.204)
- Leigh, N., Sills, A., & Knigge, C. 2011, *MNRAS*, 416, 1410, doi: [10.1111/j.1365-2966.2011.19136.x](https://doi.org/10.1111/j.1365-2966.2011.19136.x)
- Liu, B., & Lai, D. 2018, *ApJ*, 863, 68, doi: [10.3847/1538-4357/aad09f](https://doi.org/10.3847/1538-4357/aad09f)
- . 2019, *MNRAS*, 483, 4060, doi: [10.1093/mnras/sty3432](https://doi.org/10.1093/mnras/sty3432)
- Lombardi, James C., J., Rasio, F. A., & Shapiro, S. L. 1996, *ApJ*, 468, 797, doi: [10.1086/177736](https://doi.org/10.1086/177736)
- Mikkola, S., & Aarseth, S. 2002, *Celestial Mechanics and Dynamical Astronomy*, 84, 343, doi: [10.1023/A:1021149313347](https://doi.org/10.1023/A:1021149313347)
- Mikkola, S., & Aarseth, S. J. 1996, *Celestial Mechanics and Dynamical Astronomy*, 64, 197, doi: [10.1007/BF00728347](https://doi.org/10.1007/BF00728347)
- Mikkola, S., & Tanikawa, K. 1999, *MNRAS*, 310, 745, doi: [10.1046/j.1365-8711.1999.02982.x](https://doi.org/10.1046/j.1365-8711.1999.02982.x)
- Moe, M., & Di Stefano, R. 2017, *ApJS*, 230, 15, doi: [10.3847/1538-4365/aa6fb6](https://doi.org/10.3847/1538-4365/aa6fb6)
- Offner, S. S. R., Moe, M., Kratter, K. M., et al. 2023, in *Astronomical Society of the Pacific Conference Series*, Vol. 534, *Protostars and Planets VII*, ed. S. Inutsuka, Y. Aikawa, T. Muto, K. Tomida, & M. Tamura, 275, doi: [10.48550/arXiv.2203.10066](https://doi.org/10.48550/arXiv.2203.10066)
- Park, D., Kim, C., Lee, H. M., Bae, Y.-B., & Belczynski, K. 2017, *MNRAS*, 469, 4665, doi: [10.1093/mnras/stx1015](https://doi.org/10.1093/mnras/stx1015)
- Perets, H. B., & Fabrycky, D. C. 2009, *ApJ*, 697, 1048, doi: [10.1088/0004-637X/697/2/1048](https://doi.org/10.1088/0004-637X/697/2/1048)

- Perets, H. B., & Kratter, K. M. 2012, *ApJ*, 760, 99, doi: [10.1088/0004-637X/760/2/99](https://doi.org/10.1088/0004-637X/760/2/99)
- Portegies Zwart, S., McMillan, S., Harfst, S., et al. 2009, *NewA*, 14, 369, doi: [10.1016/j.newast.2008.10.006](https://doi.org/10.1016/j.newast.2008.10.006)
- Preto, M., & Tremaine, S. 1999, *AJ*, 118, 2532, doi: [10.1086/301102](https://doi.org/10.1086/301102)
- Randall, L., & Xianyu, Z.-Z. 2018, *ApJ*, 864, 134, doi: [10.3847/1538-4357/aad7fe](https://doi.org/10.3847/1538-4357/aad7fe)
- Rantala, A., Naab, T., Rizzuto, F. P., et al. 2023, *MNRAS*, 522, 5180, doi: [10.1093/mnras/stad1360](https://doi.org/10.1093/mnras/stad1360)
- Rantala, A., Pihajoki, P., Mannerkoski, M., Johansson, P. H., & Naab, T. 2020, *MNRAS*, 492, 4131, doi: [10.1093/mnras/staa084](https://doi.org/10.1093/mnras/staa084)
- Rastello, S., Amaro-Seoane, P., Arca-Sedda, M., et al. 2019, *MNRAS*, 483, 1233, doi: [10.1093/mnras/sty3193](https://doi.org/10.1093/mnras/sty3193)
- Rein, H., Hernandez, D. M., Tamayo, D., et al. 2019, *MNRAS*, 485, 5490, doi: [10.1093/mnras/stz769](https://doi.org/10.1093/mnras/stz769)
- Rodriguez, C. L., Chatterjee, S., & Rasio, F. A. 2016a, *PhRvD*, 93, 084029, doi: [10.1103/PhysRevD.93.084029](https://doi.org/10.1103/PhysRevD.93.084029)
- Rodriguez, C. L., Haster, C.-J., Chatterjee, S., Kalogera, V., & Rasio, F. A. 2016b, *ApJL*, 824, L8, doi: [10.3847/2041-8205/824/1/L8](https://doi.org/10.3847/2041-8205/824/1/L8)
- Samsing, J., Askar, A., & Giersz, M. 2018a, *ApJ*, 855, 124, doi: [10.3847/1538-4357/aaab52](https://doi.org/10.3847/1538-4357/aaab52)
- Samsing, J., & D’Orazio, D. J. 2018, *MNRAS*, 481, 5445, doi: [10.1093/mnras/sty2334](https://doi.org/10.1093/mnras/sty2334)
- Samsing, J., D’Orazio, D. J., Askar, A., & Giersz, M. 2018b, arXiv e-prints, arXiv:1802.08654, doi: [10.48550/arXiv.1802.08654](https://doi.org/10.48550/arXiv.1802.08654)
- Samsing, J., Hendriks, K., Zwick, L., D’Orazio, D. J., & Liu, B. 2024, arXiv e-prints, arXiv:2403.05625, doi: [10.48550/arXiv.2403.05625](https://doi.org/10.48550/arXiv.2403.05625)
- Sana, H., de Mink, S. E., de Koter, A., et al. 2012, *Science*, 337, 444, doi: [10.1126/science.1223344](https://doi.org/10.1126/science.1223344)
- Sills, A., Adams, T., & Davies, M. B. 2005, *MNRAS*, 358, 716, doi: [10.1111/j.1365-2966.2005.08809.x](https://doi.org/10.1111/j.1365-2966.2005.08809.x)
- Tanikawa, A. 2013, *MNRAS*, 435, 1358, doi: [10.1093/mnras/stt1380](https://doi.org/10.1093/mnras/stt1380)
- Tiwari, A., Vijaykumar, A., Kapadia, S. J., Fragione, G., & Chatterjee, S. 2024, *MNRAS*, 527, 8586, doi: [10.1093/mnras/stad3749](https://doi.org/10.1093/mnras/stad3749)
- Trani, A. A., & Spera, M. 2023, in *The Predictive Power of Computational Astrophysics as a Discover Tool*, ed. D. Bisikalo, D. Wiebe, & C. Boily, Vol. 362, 404–409, doi: [10.1017/S1743921322001818](https://doi.org/10.1017/S1743921322001818)
- Wang, L., Fujii, M. S., & Tanikawa, A. 2021, *MNRAS*, 504, 5778, doi: [10.1093/mnras/stab1157](https://doi.org/10.1093/mnras/stab1157)
- Wang, L., Iwasawa, M., Nitadori, K., & Makino, J. 2020a, *MNRAS*, 497, 536, doi: [10.1093/mnras/staa1915](https://doi.org/10.1093/mnras/staa1915)
- Wang, L., & Nitadori, K. 2020, *MNRAS*, 497, 4384, doi: [10.1093/mnras/staa2295](https://doi.org/10.1093/mnras/staa2295)
- Wang, L., Nitadori, K., & Makino, J. 2020b, *MNRAS*, 493, 3398, doi: [10.1093/mnras/staa480](https://doi.org/10.1093/mnras/staa480)
- Weatherford, N. C., Fragione, G., Kremer, K., et al. 2021, *ApJL*, 907, L25, doi: [10.3847/2041-8213/abd79c](https://doi.org/10.3847/2041-8213/abd79c)
- Wisdom, J., & Holman, M. 1991, *AJ*, 102, 1528, doi: [10.1086/115978](https://doi.org/10.1086/115978)
- Yoshida, H. 1990, *Physics Letters A*, 150, 262, doi: [10.1016/0375-9601\(90\)90092-3](https://doi.org/10.1016/0375-9601(90)90092-3)